Uric acid priming in human monocytes is driven by the AKT–PRAS40 autophagy pathway

Tania O. Crişan[a,b,c], Maartje C. P. Cleophas[a,b], Boris Novakovic[b,d], Kathrin Erler[a,b], Frank L. van de Veerdonk[a,b], Hendrik G. Stunnenberg[b,d], Mihai G. Netea[a,b,e], Charles A. Dinarello[a,b,f,1], and Leo A. B. Joosten[a,b,c,1]

[a]Department of Internal Medicine, Radboud University Medical Center, 6525 GA Nijmegen, The Netherlands; [b]Radboud Institute for Molecular Life Sciences, Radboud University Medical Center, 6525 GA Nijmegen, The Netherlands; [c]Department of Medical Genetics, Iuliu Hatieganu University of Medicine and Pharmacy, 400349 Cluj-Napoca, Romania; [d]Department of Molecular Biology, Faculty of Science, Radboud University, 6525 GA Nijmegen, The Netherlands; [e]Human Genomics Laboratory, University of Medicine and Pharmacy of Craiova, 200349 Craiova, Romania; and [f]Department of Medicine, University of Colorado Denver, Aurora, CO 80045

Contributed by Charles A. Dinarello, April 14, 2017 (sent for review December 22, 2016; reviewed by Patrick Durez and Pascal Richette)

Metabolic triggers are important inducers of the inflammatory processes in gout. Whereas the high serum urate levels observed in patients with gout predispose them to the formation of monosodium urate (MSU) crystals, soluble urate also primes for inflammatory signals in cells responding to gout-related stimuli, but also in other common metabolic diseases. In this study, we investigated the mechanisms through which uric acid selectively lowers human blood monocyte production of the natural inhibitor IL-1 receptor antagonist (IL-1Ra) and shifts production toward the highly inflammatory IL-1β. Monocytes from healthy volunteers were first primed with uric acid for 24 h and then subjected to stimulation with lipopolysaccharide (LPS) in the presence or absence of MSU. Transcriptomic analysis revealed broad inflammatory pathways associated with uric acid priming, with NF-κB and mammalian target of rapamycin (mTOR) signaling strongly increased. Functional validation did not identify NF-κB or AMP-activated protein kinase phosphorylation, but uric acid priming induced phosphorylation of AKT and proline-rich AKT substrate 40 kDa (PRAS 40), which in turn activated mTOR. Subsequently, Western blot for the autophagic structure LC3-I and LC3-II (microtubule-associated protein 1A/1B-light chain 3) fractions, as well as fluorescence microscopy of LC3-GFP–overexpressing HeLa cells, revealed lower autophagic activity in cells exposed to uric acid compared with control conditions. Interestingly, reactive oxygen species production was diminished by uric acid priming. Thus, the Akt–PRAS40 pathway is activated by uric acid, which inhibits autophagy and recapitulates the uric acid-induced proinflammatory cytokine phenotype.

uric acid | interleukin-1 | interleukin-1 receptor antagonist | AKT | autophagy

Uric acid is a naturally occurring product of purine metabolism. The elevation of serum uric acid levels above the threshold of 0.36 mM is called hyperuricemia (1). Hyperuricemia is the single necessary condition that is significantly associated with gout susceptibility and pathogenesis (2). This is due to the fact that uric acid precipitates to form monosodium urate (MSU) crystals (3), which in turn promote inflammation and arthritic events.

Due to the evolutionary loss of uricase gene functionality, uric acid is the end-product of purine metabolism in humans and higher primates (4). In less evolved organisms, uricase enzyme activity is preserved, enabling uric acid catabolism to the more soluble product allantoin (4). A relatively recent study described that the loss of uricase activity happened gradually during evolution, allowing adaptation to progressively less enzymatic activity and the slow rise of uric acid levels in the blood (5). Moreover, 90% of the total filtered urate is reabsorbed in the kidney by the uric acid transporter machinery (6). In line with this, the strongest genetic associations with hyperuricemia and gout come from variants in genes encoding urate transporters (7, 8).

The existence of these complementary mechanisms that conserve uric acid is indicative of evolutionary advantages of high uric acid levels in the blood (9, 10). Nevertheless, an increasing body of evidence highlights the role of uric acid in diseases such as chronic kidney disease (11), fatty liver disease (12), cardiorenal syndrome and hypertension (13, 14), coronary heart disease (15, 16), type 2 diabetes (17), aging (18), and cancer (19), in addition to gout. The many associations of uric acid with common inflammatory diseases lead to a scenario of thrifty genes that currently predispose to fat storage disorders and systemic comorbidities (20).

Inflammatory processes induced by uric acid are initiated after cellular injury and death, causing purines and purine degradation products to be released in the extracellular milieu (21, 22). Uric acid and MSU act as damage-associated molecular patterns (DAMPs) and induce sterile inflammation in the involved tissue (21, 22). For a long time, uric acid was considered a nonfunctional byproduct associated with metabolic syndrome, but in the context of increasing numbers of studies investigating the direct effects of uric acid in inflammation and disease pathogenesis, the quest for targetable mechanisms in uric acid-mediated inflammation has been reappraised (23).

Recently, our group has discovered that soluble uric acid exerts proinflammatory properties through a direct effect on human primary peripheral blood mononuclear cells (PBMCs) (24). We have found that PBMCs of patients with hyperuricemia produce higher amounts of proinflammatory cytokines than healthy controls after ex vivo stimulation, but the mechanisms

Significance

Hyperuricemia is a metabolic condition intrinsic to gout pathogenesis but also associated with other common metabolic inflammatory diseases. The soluble uric acid-induced priming of monocytes determines a unique shift in cytokine production consisting of high interleukin (IL)-1β but low IL-1 receptor antagonist (IL-1Ra). We investigated metabolic sensors and scanned for transcriptomic pathways and kinase activation to provide mechanistic leads for this process. We describe that uric acid suppresses autophagy and diminishes the antiinflammatory capacity of the cell. The consequences of uric acid exposure are broad and can impact a larger spectrum of inflammatory diseases from gout to metabolic, renal, or cardiovascular diseases or cancer.

Author contributions: T.O.C., H.G.S., M.G.N., C.A.D., and L.A.B.J. designed research; T.O.C., M.C.P.C., B.N., K.E., F.L.v.d.V., and L.A.B.J. performed research; F.L.v.d.V., H.G.S., C.A.D., and L.A.B.J. contributed new reagents/analytic tools; T.O.C., M.C.P.C., B.N., K.E., C.A.D., and L.A.B.J. analyzed data; and T.O.C., M.C.P.C., B.N., H.G.S., M.G.N., C.A.D., and L.A.B.J. wrote the paper.

Reviewers: P.D., Cliniques Universitaires Saint Luc, Universite Catholique de Louvain; and P.R., INSERM U1132 and University Paris-Diderot.

The authors declare no conflict of interest.

[1]To whom correspondence may be addressed. Email: leo.joosten@radboudumc.nl or Cdinare333@aol.com.

This article contains supporting information online at www.pnas.org/lookup/suppl/doi:10.1073/pnas.1620910114/-/DCSupplemental.

responsible for this inflammatory imbalance are not elucidated (24, 25). In the present study, we report the intracellular mechanisms that underlie uric acid priming effects in human monocytes.

Results

Monocytes Show a Shift Between IL-1β and IL-1Ra Production After Uric Acid Exposure. Modulatory effects of soluble uric acid on cytokine production have been previously described (24). Here we reproduce the cytokine responses induced by uric acid in a highly pure human monocyte population (Fig. S1), obtained using sequential steps of Ficoll density gradient centrifugation, Percol density gradient centrifugation, and magnetic microbeads negative selection. Monocytes were subjected to a priming protocol consisting of 24 h of exposure to medium containing increasing concentrations of solubilized uric acid, followed by washout and stimulation with lipopolysaccharide (LPS) or LPS and MSU crystals. Cytokines were measured after 24 h of priming and at the end of the experiment. Uric acid priming induced higher IL-1β production, which was visible only after restimulation with LPS or LPS + MSU, whereas IL-1β could not be measured in supernatants of cells after uric acid priming alone (Fig. 1*A*). IL-1 receptor antagonist (IL-1Ra) production showed an opposite trend compared with IL-1β, as uric acid down-regulated IL-1Ra (Fig. 1*B*). This phenotype was visible after uric acid treatment alone, and it also persisted at 48 h, following LPS + MSU stimulation. Allantoin used as a control priming stimulus was not able to induce any of these effects (Fig. 1 *A* and *B*).

Transcriptomic Data Reveal Broad Functional Effects of Uric Acid in Monocytes and Show Enrichment in Candidate Pathways in IL-1 Regulation. To extract mechanistic information to explain the inflammatory effects of uric acid, RNA-sequencing was performed in highly purified monocytes (separated by negative selection). Efficacy of monocyte selection was assessed by flow cytometry (Fig. S1). The experimental setup is summarized in Fig. 2*A*. Monocytes were exposed to medium or 50 mg/dL uric acid for 20 h followed by stimulation with medium or LPS 10 ng/mL for another 4 h (cytokines were measured in the supernatants of cells used for RNA-sequencing; Fig. S1), and RNA-sequencing was performed in fresh monocytes and 24-h samples. Known cytokine and mRNA patterns for *IL1B*, *IL1RN*, and *IL6* were confirmed by RNA-sequencing (Fig. 2 *B–D*). Principal component analysis (PCA) shows moderate effects of uric acid in its capacity to segregate the samples (~8% of variance explained by PC2), and genes that contribute to PC2 were extracted for further pathway enrichment analysis; of note, *EIF4EBP3* is up-regulated in uric acid-treated samples, suggesting implications of the mTOR pathway in uric acid effects (Fig. 2*E*). Pathway enrichment analysis was performed using the Kyoto Encyclopedia of Genes and Genomes (KEGG) pathway database starting from significantly regulated genes (full list depicted in Table S1) to top 100 contributors to PC2 (Fig. 2*E*). Gene ontology (GO) terms associated with up-regulated and down-regulated genes are depicted in Fig. S2. The analysis shows enrichment in pathways involving innate immunity, cytokine, and chemokine interactions; Toll-like receptor signaling; as well as pathways that could indicate mechanistic leads in uric acid-induced proinflammatory status. Focusing on possible targets regulating IL-1β/IL-1Ra in response to uric acid, terms such as NF-κB were highlighted in both down-regulated and up-regulated gene analysis, indicating that this was a common term associated with the general process and less likely to explain the shift in cytokines. Other pathways that were relevant in the context of uric acid signaling, such as FoxO (transcription factors downstream of AKT), or lysosomal-mediated processes were indicative of intracellular pathways that are involved in modulating IL-1β production and were further explored. A full list of GO terms and significance coefficients as well as genes associated with the terms for up-regulated genes are presented in Table S2.

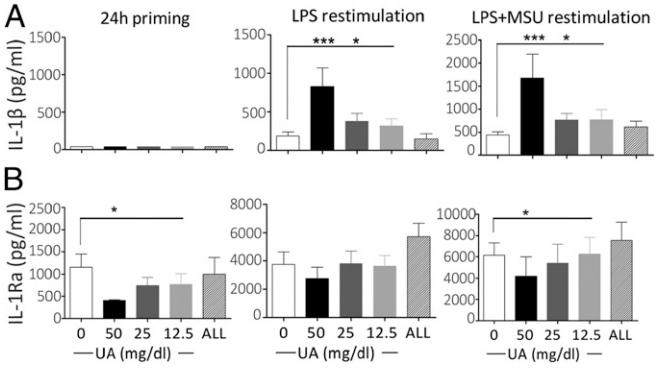

Fig. 1. Enhanced IL-1β and diminished IL-1Ra production in uric acid-primed monocytes. Monocytes were freshly isolated by differential centrifugation and magnetic beads negative selection and were stimulated in vitro with increasing concentrations of uric acid solubilized in RPMI supplemented with 10% human serum. Monocytes were exposed to increasing concentrations of uric acid (UA), 50 mg/dL allantoin (ALL), or medium alone for 24 h (24 h priming). Afterward, the medium was refreshed and the cells were stimulated with 10 ng/mL LPS or LPS + 300 μg/mL MSU crystals for another 24 h. IL-1β (*A*) and IL-1Ra (*B*) cytokine production in the supernatant of cells was measured by ELISA after 24 h of priming and after another 24 h of stimulation. Data are shown as means ± SEM of at least six donors from three independent experiments; data were analyzed using Friedman test. $*P < 0.05$, $***P < 0.001$.

AKT Is Phosphorylated in Uric Acid-Primed Monocytes in the Absence of Reactive Oxygen Species Induction. To describe the intracellular signaling related to uric acid priming, we sought to validate targets revealed by the transcriptomic analysis. The involvement of NF-κB in uric acid priming effects was assessed by Western blot of phosphorylated p65. Uric acid (50 mg/dL) was unable to modify phosphorylated p65 levels after 30 min, 1 h, or 2 h (Fig. S3). This suggests that NF-κB is associated with the transcription of genes involved in general inflammatory processes, explaining its appearance as a common hit in transcriptomic data (Fig. S2), but is not likely directly activating and mediating the IL-1β–shifted production pattern.

Additional targets indicated by the transcriptomic analysis were the terms mTOR (up-regulated) and FoxO (down-regulated), both downstream of AKT. AKT has been associated previously with effects of uric acid, such as oxidative stress and AKT inhibition, which could be an explanation for reduced IL-1Ra (26). Uric acid has also been linked to AMP-activated protein kinase (AMPK) inhibition through reactive oxygen species (ROS) induction, and this effect was described as inducing mTOR (27). We have investigated these pathways in human monocytes. The dependence of uric acid effects on ROS production has been studied by measurement of ROS using a Luminol-based assay and in PBMCs of a patient with chronic granulomatous disease (CGD). Uric acid costimulation diminished ROS production, as measured by 1-h kinetics in response to zymosan or phorbol-12-mystrate-13-acetate (PMA) stimulation (receptor-dependent and receptor-independent ROS induction, respectively) (Fig. 3 *A* and *B*). CGD patients have NADPH oxidase mutations leading to an inability to produce cytosolic ROS. To determine whether ROS are required for uric acid modulation of cytokines, the priming setup was applied on PBMCs isolated from a CGD patient and one healthy subject. Uric acid could still prime production of IL-1β (Fig. 3*C*) and reduction of IL-1Ra (Fig. S4), indicating that these effects do not require cytosolic ROS production.

Phosphorylation of AMPK and AKT was assessed by Western blot in cells treated with inducers of AMPK (Metformin or AICAR) or AKT (β-glucan or insulin), respectively (Fig. 3 *D* and *E*). AMPK was not modified by uric acid treatment. In contrast, uric

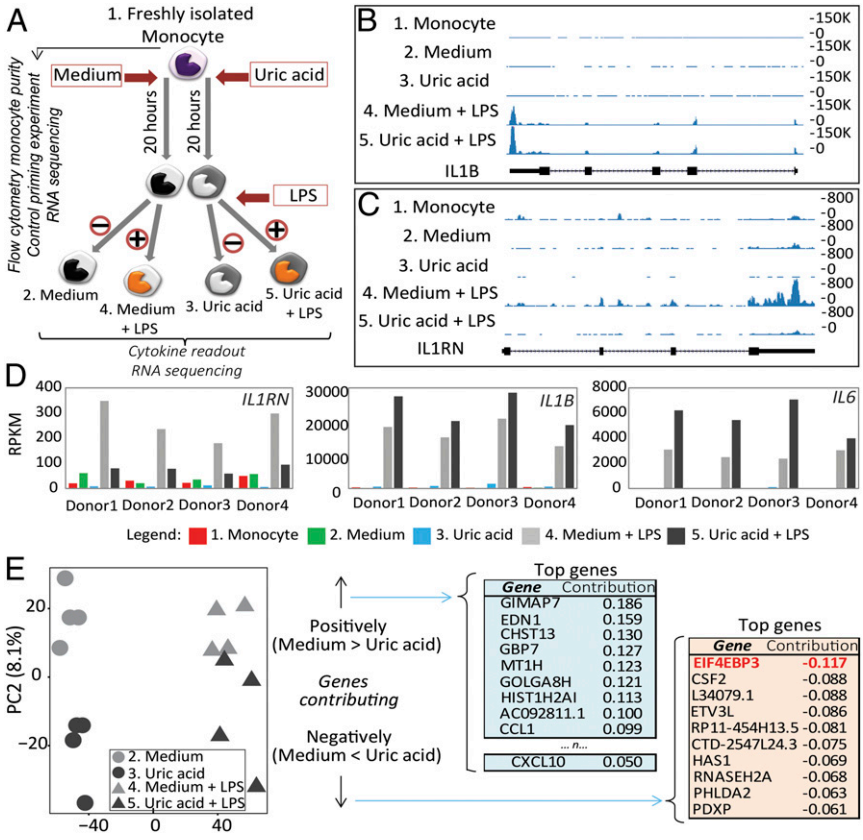

Fig. 2. Transcriptomic analysis in uric acid-primed monocytes. Monocytes were enriched using sequential steps of Ficoll density gradient centrifugation, Percol density gradient centrifugation, and negative selection using magnetic beads. Cells were exposed to 50 mg/dL medium or uric acid for 20 h followed by stimulation with medium or 10 ng/mL LPS for another 4 h, and RNA sequencing was performed in fresh monocytes (sample 1) and 24-h samples (samples 2–5) (*A*). Example UCSC genome browser screenshot of a single donor at *IL1B* (*B*) and *IL1RN* (*C*) gene tracks showing higher *IL1B* peaks and lower *IL1RN* peaks in uric acid samples versus control (sample 3 versus sample 2, or samples 5 versus sample 4). (*D*) Plots depicting RPKM (reads per kilobase per million mapped reads) values (from *Left* to *Right*) for *IL1RN*, *IL1B*, and *IL6* genes showing that normalized read counts are lower for *IL1RN* and higher for *IL1B* and *IL6* in uric acid-treated samples compared with controls. (*E*) PCA of samples at day 1 shows segregation of control samples from uric acid-treated samples; genes that contribute to PC2 were extracted for further pathway enrichment analysis (positive contribution refers to genes that are up-regulated in medium control compared with uric acid, thus down-regulated in uric acid samples, and vice versa for negatively contributing genes).

acid priming induced phosphorylated AKT in the monocytes (Fig. 3*E*). This effect of AKT induction was observed in a time-dependent manner and was reversible using the phosphatidyl-inositol 3 kinase (PI3K) inhibitor wortmannin (Fig. 3*F* and Fig. S5).

AKT–PRAS40 Transduces Effects to Autophagy Inhibition, Which in Turn Recapitulates the Uric Acid-Induced Cytokine Pattern. To further determine which signaling pathway is important for uric acid inflammatory effects, phosphokinase activity was scanned in monocytes using a human proteome profiler–phosphokinase array (R&D), and percent change of spotted proteins was calculated. Consistently throughout the three experiments performing this assay, PRAS40 (proline-rich AKT substrate 40 kDa) was identified as being phosphorylated by uric acid (Fig. S6). This was further validated by Western blot in a similar experimental setup (Fig. 4*A*).

It is known that PRAS40 phosphorylation has an inhibitory effect on regulatory-associated protein of mTOR (Raptor). Raptor dissociates from mTOR complex 1 and induces mTOR (28), which in turn has inhibitory effects on autophagy. The effects of uric acid on autophagy were investigated using complementary assays in HeLa cells. HeLa cells overexpressing LC3 coupled with GFP were stimulated with rapamycin in the presence or absence of uric acid. Green fluorescent punctae were microscopically assessed to determine autophagy activity (Fig. 4*B*). Higher numbers of punctae were visible after positive autophagy control rapamycin, and this was inhibited by uric acid (Fig. 4*B*). Western blot assessment of endogenous production of the LC3 autophagy marker in response to the same treatments depicted similar inhibitory effects of uric acid on LC3-II levels (lower band, migrates faster) compared with LC3-I (migrates slower than the lipidated LC3-II) (Fig. 4*C*). To observe whether uric acid inhibition could explain the uric acid-specific cytokine pattern involving induction of IL-1β and repression of IL-1Ra, pharmacological inhibitors of autophagy were used to recapitulate uric acid effects. Inhibition of autophagy by PI3K inhibitors 3-methyl adenine (3MA) or wortmannin is known to significantly enhance IL-1β, as previously demonstrated (29, 30), whereas IL-1Ra was reduced (Fig. 4*D*), enforcing that this signaling pathway is likely mediating the effects on cytokine production by uric acid priming.

Uricase Inhibition in Mice Potentiates Joint Inflammation in an in Vivo Model of Gout. To further explore the effects of high uric acid levels on inflammation in gout, an in vivo model of hyperuricaemia in mice was used. Mice were administered exogenous uric acid in addition to oxonic acid (uricase inhibitor) to promote hyperuricemia and were given intra-articular (i.a.) injections with MSU crystals and palmitic acid (C16) to induce gout. Inflammation was significantly enhanced in the oxonic acid group compared with controls as observed by macroscopic scoring of joints and histology (Fig. 5).

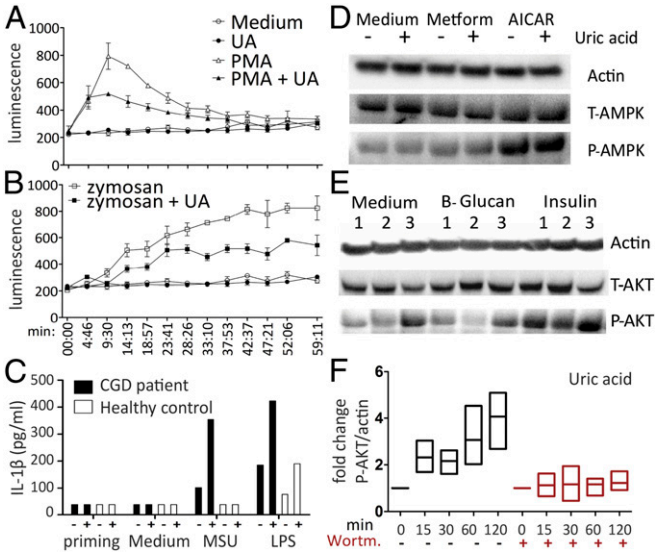

Fig. 3. Phosphorylation of AKT and lack of ROS or AMPK induction by uric acid. Percol-enriched monocytes (10^5 per well) were stimulated with 50 μg/mL Zymosan (*A*) or 250 ng/mL PMA (*B*) to induce receptor-dependent or receptor-independent ROS production, in the presence or absence of 50 mg/dL uric acid. Kinetics of ROS production was documented for 1 h and is representative of two independent experiments using five donors. (*C*) PBMCs of a CGD patient and control were isolated, and 0.5×10^6 cells were stimulated per well with 300 μg/mL MSU or 10 ng/mL LPS after priming with medium or uric acid, and IL-1β levels were measured. (*D*) The 10^6 monocytes were prestimulated with medium or AMPK inducers such as 30 mM Metformin or 0.5 mM AICAR, followed by 2 h in the presence or absence of 50 mg/dL uric acid. (*E*) Monocytes were prestimulated with medium or AKT inducers such as 5 μg/mL β-glucan or 100 nM insulin, followed by 2 h in the presence or absence of 100 nM wortmannin (AKT inhibitor) or 50 mg/dL uric acid. (*F*) The 10^6 monocytes were treated with 50 mg/dL uric acid for increasing durations in the presence or absence of 100 nM wortmannin in four donors.

Discussion

In the current study, we investigated the mechanisms through which uric acid primes human monocytes. The previous findings that higher concentrations of uric acid promote IL-1 production and inhibit IL-1Ra synthesis were confirmed. This uric acid effect is unique because it shifts the IL-1/IL-1Ra balance to a proinflammatory phenotype by strong reduction of IL-1Ra through a yet-unclear mechanism. Very high concentrations of uric acid have been used in this setup and previously (24) to obtain the maximum effect and allow in vitro manipulation. Although we cannot exclude that uric acid microcrystals that were undetectable by polarized light microscopy are also involved in this effect, we see a clearly distinct pattern of cytokines induced by soluble uric acid compared with MSU crystals (which in turn induce both IL-1β and IL-1Ra) (Fig. 1).

We generated transcriptomic data through RNA-sequencing in highly pure human monocytes after 24 h of treatment with medium or uric acid. LPS stimulation for 4 h was used to boost the potential differences observed between medium and uric acid exposure. As summarized in Fig. 2 *B*–*D*, the expected effects could be demonstrated in RNA-sequencing samples: *IL1B* and *IL6* RNA levels were higher in uric acid compared with medium control after 24 h; *IL1RN* RNA levels were lower in uric acid compared with medium control after 24 h; and these differences were amplified by LPS stimulation. This was in line with cytokine data (Fig. 1) showing that uric acid effects are not visible unless cells are challenged with a pattern-recognition receptor ligand, such as LPS. PCA (Fig. 2*E*) revealed a moderate effect of uric acid in segregating the 24-h samples, with most of the variance being attributable to LPS. This effect is also not surprising, as LPS determines a strong transcriptional program, whereas uric acid had a less dramatic but highly consistent effect.

Pathway enrichment analysis was performed using the KEGG database using: genes that varied significantly in uric acid compared with medium control at 24 h (Table S1), and top genes that made a contribution to PC2 (Fig. 2*E*). The analysis revealed the enrichment of several pathways (Fig. S2 and Table S2). Pathways providing mechanistic links for modulating cytokine production (NF-κB, mTOR, FoxO, lysosome) were further investigated. Uric acid was previously reported to induce NF-κB and to promote cell death in pancreatic β cells (31). In our in vitro setup, we were unable to detect changes in phosphorylation of NF-κB component p65 in monocytes treated with uric acid (Fig. S3), indicating that NF-κB is likely a common term associated with the cytokine genes regulated by uric acid and not reflecting its mechanism of action.

We further investigated the AKT pathway, which was indicated by RNA-sequencing data through the up-regulated mTOR signaling pathway and down-regulated FoxO signaling pathway (Fig. S2). AKT has also been studied in relation to uric acid effects in a model of potassium oxonate-induced hyperuricemia in mice. AKT phosphorylation was inhibited by uric acid, and this diminished insulin sensitivity in cardiomyocytes (32) and in liver cells (26) through an ROS-dependent pathway. In our experimental setup, uric acid potently inhibited ROS production (Fig. 3 *A* and *B*) and could still prime the cells for high IL-1β and low IL-1Ra in cells of CGD patients (Fig. 3*C* and Fig. S4). These findings exclude a NADPH oxidase-dependent mechanism for the observed findings and demonstrate an antioxidant role of uric acid in human primary monocytes. This finding adds information to existing evidence showing the dual role of uric acid in oxidative stress (20). In line with our findings, a study investigating the expression of NF-κB p65 and NADPH oxidase $p47^{phox}$ in brachial artery endothelial cells found no correlation with serum uric acid levels (33). Moreover, AKT was induced by uric acid (Fig. 3 *E* and *F*), making AKT an important player in uric acid signal transduction. Whereas the induction of ROS in other studies also led to AMPK inhibition (27, 34), our

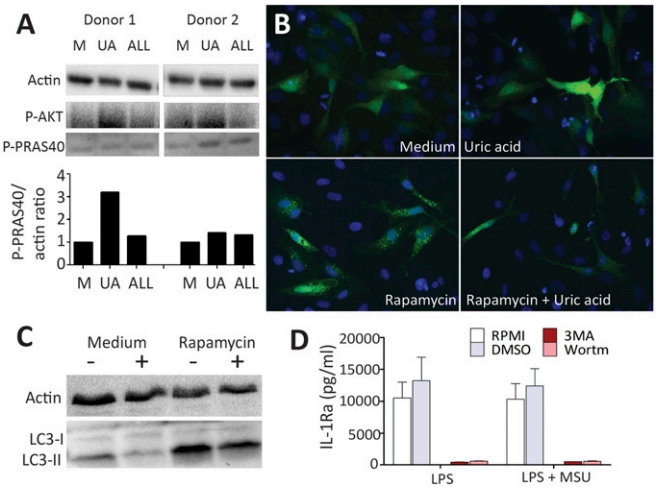

Fig. 4. Identification of PRAS40 as intermediate in AKT signal transduction to inhibit autophagy in uric acid-primed cells. Negatively selected monocytes were primed with or without uric acid (UA) or allantoin (ALL) for 24 h, followed by 7 min of short exposure to high concentrations of 1 μg/mL LPS. (*A*) Cells were lysed and PRAS40 was identified through Western blot. (*B*) The effects of downstream PRAS40 and mTOR activation on autophagy were examined by means of fluorescence microscopy in HeLa cells overexpressing LC3 coupled with GFP (original magnification, 200×) (*B*) and by Western blotting for LC3-I and LC3-II in HeLa cells (*C*). (*D*) Fresh PBMCs were stimulated with 10 ng/mL LPS or LPS + 300 μg/mL MSU in the presence or absence of autophagy inhibitors 3MA (10 mM) and wortmannin (100 nM).

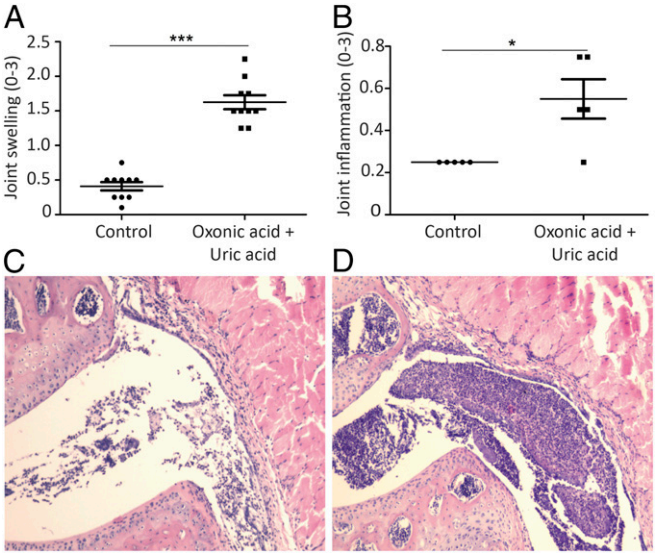

Fig. 5. Uricase inhibition in mice exacerbates joint inflammation in a model of acute gout arthritis. Macroscopic (*A*) and microscopic (*B*) scores of the knees in mice treated with vehicle control or oxonic acid + uric acid following i.a. injection of MSU + C16. Histology (H&E staining) of joints treated with MSU + C16 in control (*C*) and oxonic acid (*D*) mice. (*A*) 10 knees per group, Mann–Whitney, ***$P < 0.001$. (*B*) 5 knees per group, Mann–Whitney, *$P < 0.05$.

assessment did not reveal changes in AMPK phosphorylation in monocytes (Fig. 3*D*), in line with the observed antioxidant effect of uric acid in our experimental setup.

Finally, we discovered that AKT induction is followed by downstream PRAS40 phosphorylation, which couples this signaling pathway to decreased LC3-II autophagosome formation in uric acid-treated HeLa cells (Fig. 4). Autophagy is a conserved housekeeping lysosomal process involving LC3 and its phosphatidyl ethanolamine lipidated form LC3-II, which has the role of degrading long-lived intracellular cargo but is also closely linked to inflammation (35). A newly characterized noncanonical pathway termed LC3-associated phagocytosis (LAP) is still difficult to dissociate from classical autophagy (36). Autophagy defects have largely been inflicted in human inflammatory diseases (37) due to processes such as inflammasome activation (38), lack of pro–IL-1β (39) degradation, or enhanced transcription of IL-1β (29). A discordance in IL-1β and IL-1Ra cytokines was described in CGD where patients are deficient in autophagy due to an inability to produce ROS (40). This deficiency in autophagy led to IL-1–mediated inflammation that could be rescued by IL-1Ra administration (40). Moreover, pharmacological inhibition of autophagy in human cells also showed down-regulation of IL-1Ra (Fig. 4*D*). This shows that autophagy inhibition is an important mechanism that can explain the high levels of IL-1β observed in uric acid-primed monocytes while uniquely discoupling IL-1 from the natural antagonist IL-1Ra. The further characterization and validation of these findings in humans in vivo is of high relevance for the regulatory mechanisms of gout. On the one hand, autophagy deficiency can lead to proinflammatory signals that increase the vulnerability of patients to stimuli that precipitate gout. On the other hand, boosting autophagy as well as restoring IL-1Ra levels can limit the degree of inflammation or facilitate the resolution of attacks.

Nevertheless, the effects on cytokine production are likely to be influenced by other pathways in addition to AKT, as revealed by other kinases such as ERK, which was phosphorylated upon uric acid treatment (Fig. S6). This diversity of uric acid-induced pathways illustrates that uric acid can impact on many different biological processes and affect different phenotypes of the cell, reflecting a large group of diseases for which hyperuricemia and DAMP-mediated responses are of relevance.

In conclusion, our data show that uric acid has complex effects in monocytes. First, it induced the phosphorylation of AKT in line with the effects of uric acid on phosphorylation of PRAS40, which is an mTOR inhibitory molecule downstream of AKT. Subsequently, activation of the AKT–PRAS40 pathway led to a decrease in LC3-II formation and less fluorescent green punctae on LC3-GFP–overexpressing HeLa cells. This coincides with diminished lysosomal-mediated pathways such as autophagy or noncanonical LAP. Moreover, autophagy blockade is known to induce higher IL-1β production and discordance between IL-1β and IL-1Ra, whereas normal autophagy activity has been associated with basal inhibition of inflammation. Finally, uricase blockade and the exogenous administration of uric acid in mice determined a higher inflammatory reaction to i.a. injection of MSU and C16, providing proof of concept that high uric acid levels can increase inflammatory responses in acute gout models in vivo.

Pathways with importance in common metabolic disorders and innate immunity implications have been highlighted by this approach and are warranted investigation in subsequent studies. The link between high uric acid exposure and autophagy is likely to be an important new susceptibility factor in conditions associated with hyperuricemia, and the validity and utility of this finding are to be assessed in future patient studies.

Materials and Methods

Volunteers. The study was approved by the Arnhem-Nijmegen ethical review board. All human experiments were conducted according to the Declaration of Helsinki. Informed written consent of each human subject was provided.

PBMC and Monocyte Isolation. PBMCs were separated using Ficoll-Paque (Pharmacia Biotech) and suspended in RPMI (Roswell Park Memorial Institute 1640). Monocytes were enriched using hyperosmotic Percol solution followed by negative selection using the Pan Monocyte Isolation kit (Miltenyi Biotec), and efficacy of selection was verified by flow cytometry.

Stimulation Experiments. Experiments were performed in culture medium containing RPMI, supplemented with 10% human pooled serum. Cells were primed for 24 h with medium, uric acid, or allantoin; cells were washed with warm PBS; and remaining adherent cells were stimulated as described. For RNA-sequencing experiments, 0.5×10^6 monocytes were seeded per well in six-well plates (Corning) and were primed for 20 h followed by addition of 10 ng/mL medium or LPS for another 4 h.

Cytokine Measurements. Cytokines were measured using ELISA kits for IL-1β and IL-1Ra (R&D Systems).

Western Blot. Western blotting was performed using a Trans Turbo Blot system (Bio-Rad) according to the manufacturer's instructions. Protein was loaded and separated on SDS/PAGE using 4–15% gradient precast gels and transferred to PVDF (polyvinylidene fluoride) membranes using the semidry method (Bio-Rad). Proteome profiler–human phosphokinase array kit (R&D Systems) was used to assess phosphokinase activity upon uric acid treatment in monocytes.

ROS Measurement. ROS formation was measured by a chemiluminescence assay using luminol over 1 h of exposure of cells to stimuli.

Fluorescence Microscopy. HeLa cells overexpressing GFP-LC3 were obtained as previously described (30). Green fluorescent punctae were observed to assess autophagy activity after uric acid stimulation.

RNA-Sequencing Preparation and Analysis. Preparation of RNA for sequencing was performed as described in ref. 41. Total RNA was extracted from cells using the Qiagen RNeasy RNA extraction kit (Qiagen). Ribosomal RNA was removed using the riboZero rRNA removal kit (Illumina), and RNA was fragmented into 200-bp fragments, followed by first- and second-strand cDNA synthesis. Library preparation was performed using the KAPA hyperprep kit (KAPA Biosystems). RNA-sequencing reads were aligned to the hg19 reference genome using bwa (42). Dynamic genes were identified using DESEQ and were

used for PCA. Genes contributing to uric acid differences were extracted using the package prcomp and were used for GO analysis.

Mouse Model. Gout arthritis was induced in mice through i.a. injection of MSU and palmitate (C16) as previously described (43, 44). Hyperuricemia was induced in mice through uricase inhibition with oxonic acid (45, 46).

Data Availability. A detailed version of this section is described in *SI Materials and Methods*. Data used for this manuscript will be made available to readers upon request.

ACKNOWLEDGMENTS. We thank Dr. Shuang-Yin Wang for initial RNA-sequencing data mapping. T.O.C. and L.A.B.J. are supported by a Competitiveness Operational Programme grant of the Romanian Ministry of European Funds (HINT, ID P_37_762; MySMIS 103587). M.C.P.C. is supported by Dutch Arthritis Foundation Grant NR-12-2-303. B.N. is supported by an NHMRC (National Health and Medical Research Council, Australia) CJ Martin Fellowship. M.G.N. was supported by ERC (European Research Council) Grant 310372, a Spinoza grant (2016), and a Competitiveness Operational Programme grant of the Romanian Ministry of European Funds (FUSE, Functional Genomics in Severe Infections 103454). C.A.D. was supported by NIH Grant AI-15614.

1. Zhang W, et al.; EULAR Standing Committee for International Clinical Studies Including Therapeutics (2006) EULAR evidence based recommendations for gout. Part I: Diagnosis. Report of a task force of the Standing Committee for International Clinical Studies Including Therapeutics (ESCISIT). *Ann Rheum Dis* 65:1301–1311.
2. Roddy E, Doherty M (2010) Epidemiology of gout. *Arthritis Res Ther* 12:223.
3. Mandel NS, Mandel GS (1976) Monosodium urate monohydrate, the gout culprit. *J Am Chem Soc* 98:2319–2323.
4. Wu XW, Muzny DM, Lee CC, Caskey CT (1992) Two independent mutational events in the loss of urate oxidase during hominoid evolution. *J Mol Evol* 34:78–84.
5. Kratzer JT, et al. (2014) Evolutionary history and metabolic insights of ancient mammalian uricases. *Proc Natl Acad Sci USA* 111:3763–3768.
6. Ichida K, et al. (2004) Clinical and molecular analysis of patients with renal hypouricemia in Japan-influence of URAT1 gene on urinary urate excretion. *J Am Soc Nephrol* 15:164–173.
7. Köttgen A, et al.; LifeLines Cohort Study; CARDIoGRAM Consortium; DIAGRAM Consortium; ICBP Consortium; MAGIC Consortium (2013) Genome-wide association analyses identify 18 new loci associated with serum urate concentrations. *Nat Genet* 45:145–154.
8. Merriman TR, Dalbeth N (2011) The genetic basis of hyperuricaemia and gout. *Join Bone Spine* 78:35–40.
9. Álvarez-Lario B, Macarrón-Vicente J (2010) Uric acid and evolution. *Rheumatology (Oxford)* 49:2010–2015.
10. Watanabe S, et al. (2002) Uric acid, hominoid evolution, and the pathogenesis of salt-sensitivity. *Hypertension* 40:355–360.
11. Johnson RJ, et al. (2013) Uric acid and chronic kidney disease: Which is chasing which? *Nephrol Dial Transplant* 28:2221–2228.
12. Sirota JC, et al. (2013) Elevated serum uric acid levels are associated with non-alcoholic fatty liver disease independently of metabolic syndrome features in the United States: Liver ultrasound data from the National Health and Nutrition Examination Survey. *Metabolism* 62:392–399.
13. Heinig M, Johnson RJ (2006) Role of uric acid in hypertension, renal disease, and metabolic syndrome. *Cleve Clin J Med* 73:1059–1064.
14. Chaudhary K, Malhotra K, Sowers J, Aroor A (2013) Uric acid—Key ingredient in the recipe for cardiorenal metabolic syndrome. *Cardiorenal Med* 3:208–220.
15. Kim SY, et al. (2010) Hyperuricemia and coronary heart disease: A systematic review and meta-analysis. *Arthritis Care Res (Hoboken)* 62:170–180.
16. Zuo T, et al. (2016) Hyperuricemia and coronary heart disease mortality: A meta-analysis of prospective cohort studies. *BMC Cardiovasc Disord* 16:207.
17. Athyros VG, Mikhailidis DP (2014) Uric acid, chronic kidney disease and type 2 diabetes: A cluster of vascular risk factors. *J Diabetes Complications* 28:122–123.
18. Feldman N, Rotter-Maskowitz A, Okun E (2015) DAMPs as mediators of sterile inflammation in aging-related pathologies. *Ageing Res Rev* 24:29–39.
19. Eisenbacher JL, et al. (2014) S100A4 and uric acid promote mesenchymal stromal cell induction of IL-10+/IDO+ lymphocytes. *J Immunol* 192:6102–6110.
20. Johnson RJ, Lanaspa MA, Gaucher EA (2011) Uric acid: A danger signal from the RNA world that may have a role in the epidemic of obesity, metabolic syndrome, and cardiorenal disease: Evolutionary considerations. *Semin Nephrol* 31:394–399.
21. Shi Y, Evans JE, Rock KL (2003) Molecular identification of a danger signal that alerts the immune system to dying cells. *Nature* 425:516–521.
22. Kono H, Chen CJ, Ontiveros F, Rock KL (2010) Uric acid promotes an acute inflammatory response to sterile cell death in mice. *J Clin Invest* 120:1939–1949.
23. Soltani Z, Rasheed K, Kapusta DR, Reisin E (2013) Potential role of uric acid in metabolic syndrome, hypertension, kidney injury, and cardiovascular diseases: Is it time for reappraisal? *Curr Hypertens Rep* 15:175–181.
24. Crişan TO, et al. (2016) Soluble uric acid primes TLR-induced proinflammatory cytokine production by human primary cells via inhibition of IL-1Ra. *Ann Rheum Dis* 75:755–762.
25. Mylona EE, et al. (2012) Enhanced interleukin-1β production of PBMCs from patients with gout after stimulation with Toll-like receptor-2 ligands and urate crystals. *Arthritis Res Ther* 14:R158.
26. Zhu Y, et al. (2014) High uric acid directly inhibits insulin signalling and induces insulin resistance. *Biochem Biophys Res Commun* 447:707–714.
27. Zhang Y, et al. (2013) Uric acid induces oxidative stress and growth inhibition by activating adenosine monophosphate-activated protein kinase and extracellular signal-regulated kinase signal pathways in pancreatic β cells. *Mol Cell Endocrinol* 375:89–96.
28. Wiza C, Nascimento EB, Ouwens DM (2012) Role of PRAS40 in Akt and mTOR signaling in health and disease. *Am J Physiol Endocrinol Metab* 302:E1453–E1460.
29. Crişan TO, et al. (2011) Inflammasome-independent modulation of cytokine response by autophagy in human cells. *PLoS One* 6:e18666.
30. Buffen K, et al. (2013) Autophagy modulates Borrelia burgdorferi-induced production of interleukin-1β (IL-1β). *J Biol Chem* 288:8658–8666.
31. Jia L, et al. (2013) Hyperuricemia causes pancreatic β-cell death and dysfunction through NF-κB signaling pathway. *PLoS One* 8:e78284.
32. Zhi L, et al. (2016) High uric acid induces insulin resistance in cardiomyocytes in vitro and in vivo. *PLoS One* 11:e0147737.
33. Jalal DI, Jablonski KL, McFann K, Chonchol MB, Seals DR (2012) Vascular endothelial function is not related to serum uric acid in healthy adults. *Am J Hypertens* 25:407–413.
34. Luo C, et al. (2016) High uric acid activates the ROS-AMPK pathway, impairs CD68 expression and inhibits OxLDL-induced foam-cell formation in a human monocytic cell line, THP-1. *Cell Physiol Biochem* 40:538–548.
35. Deretic V (2016) Autophagy in leukocytes and other cells: Mechanisms, subsystem organization, selectivity, and links to innate immunity. *J Leukoc Biol* 100:969–978.
36. Martinez J, et al. (2015) Molecular characterization of LC3-associated phagocytosis reveals distinct roles for Rubicon, NOX2 and autophagy proteins. *Nat Cell Biol* 17:893–906.
37. Netea-Maier RT, Plantinga TS, van de Veerdonk FL, Smit JW, Netea MG (2016) Modulation of inflammation by autophagy: Consequences for human disease. *Autophagy* 12:245–260.
38. Zhong Z, Sanchez-Lopez E, Karin M (2016) Autophagy, NLRP3 inflammasome and auto-inflammatory/immune diseases. *Clin Exp Rheumatol* 34(4, Suppl 98):12–16.
39. Harris J, et al. (2011) Autophagy controls IL-1beta secretion by targeting pro-IL-1beta for degradation. *J Biol Chem* 286:9587–9597.
40. de Luca A, et al. (2014) IL-1 receptor blockade restores autophagy and reduces inflammation in chronic granulomatous disease in mice and in humans. *Proc Natl Acad Sci USA* 111:3526–3531.
41. Novakovic B, et al. (2016) beta-glucan reverses the epigenetic state of LPS-induced immunological tolerance. *Cell* 167:1354–1368 e1314.
42. Li H, Durbin R (2009) Fast and accurate short read alignment with Burrows-Wheeler transform. *Bioinformatics* 25:1754–1760.
43. Joosten LA, et al. (2010) Engagement of fatty acids with Toll-like receptor 2 drives interleukin-1β production via the ASC/caspase 1 pathway in monosodium urate monohydrate crystal-induced gouty arthritis. *Arthritis Rheum* 62:3237–3248.
44. Joosten LA, et al. (2016) Alpha-1-anti-trypsin-Fc fusion protein ameliorates gouty arthritis by reducing release and extracellular processing of IL-1β and by the induction of endogenous IL-1Ra. *Ann Rheum Dis* 75:1219–1227.
45. Dankers AC, et al. (2013) Hyperuricemia influences tryptophan metabolism via inhibition of multidrug resistance protein 4 (MRP4) and breast cancer resistance protein (BCRP). *Biochim Biophys Acta* 1832:1715–1722.
46. Patschan D, Patschan S, Gobe GG, Chintala S, Goligorsky MS (2007) Uric acid heralds ischemic tissue injury to mobilize endothelial progenitor cells. *J Am Soc Nephrol* 18:1516–1524.
47. Repnik U, Knezevic M, Jeras M (2003) Simple and cost-effective isolation of monocytes from buffy coats. *J Immunol Methods* 278:283–292.